The Ultraviolet Photochemistry of Diacetylene with Styrene

Allison G. Robinson, Paul R. Winter, and Timothy S. Zwier*

Department of Chemistry, Purdue University, West Lafayette, Indiana 47907-1393

Received: December 12, 2001

The reaction of metastable diacetylene with styrene is explored using a molecular beam pump−probe time-of-flight (TOF) mass spectrometer. Diacetylene is laser-excited to the $2^1_0 6^1_0$ band of the $^1\Delta_u \leftarrow X^1\Sigma^+_g$ transition, whereupon rapid intersystem crossing occurs to the lowest triplet states. The triplet state diacetylene then reacts with styrene as the gas mixture traverses a short reaction tube (∼20 μs). The reaction is quenched as the gas mixture expands into a vacuum where the primary photoproducts are probed using vacuum ultraviolet (VUV) photoionization, resonant two-photon ionization (R2PI), and UV−UV holeburning. The major products from the reaction have molecular formulas $C_{10}H_8$, $C_{12}H_8$, and $C_{12}H_9$. Two different $C_{10}H_8$ products have been identified as 1-phenyl-1-buten-3-yne and m-ethynyl styrene using UV−UV holeburning and comparing with spectra of authentic samples. Mechanisms for the formation of the above products are proposed on the basis of deuterium substitution studies of the reaction. The potential implications of these reactions for the formation of polycyclic aromatic hydrocarbons in sooting flames is discussed.

I. Introduction

Diacetylene (C_4H_2, H−C≡C−C≡C−H) is one of the most abundant C4 species in flames, and thus plays an important role in current models of flames.[1−4] Among the notable characteristics of diacetylene is its strong chemical bonds, which hinder dissociation to form free radicals. The weakest bond in C_4H_2 is the acetylenic C−H bond, with a bond dissociation energy of almost 130 kcal/mol.[5] As a result, C_4H_2 undergoes molecular rather than radical reactions in moderate-temperature flames.[6] As the first member of the poly-yne series, C_4H_2 is known to have long-lived triplet states only 60 and 72 kcal/mol above the ground state.[7] These states have the potential to contribute to the chemical reactivity of C_4H_2 in various environments, including flames.

In an attempt to understand the chemistry of triplet state diacetylene (hereafter C_4H_2*), we have conducted a systematic study of C_4H_2* with several small hydrocarbons commonly found in flames.[8−12] In earlier studies, larger poly-yne, cumulene, and enyne species were formed. Even more intriguing, in the reaction of C_4H_2* with 1,3-butadiene, the dominant products are the prototypical aromatics benzene and phenylacetylene.[12] Thus, C_4H_2* can form benzene in a single bimolecular reaction with 1,3-butadiene without the formation of free radicals.

The recent flame study of McEnally et al.[13] showed that small amounts of diacetylene doped into a methane/air flame produce substantial increases in benzene and phenyl-acetylene concentrations, and dramatic increases in the amount of soot in the flame. However, when both diacetylene and 1,3-butadiene were codoped into the flame, little synergistic enhancement of the aromatic concentrations were found, suggesting that the C_4H_2* + 1,3-butadiene reaction was not a dominant contributor to the aromatic concentrations in this flame.

While such studies are shedding light on the routes to the formation of the first ring,[14,15] attention is increasingly turning to the subsequent steps that lead from benzene to polyaromatic hydrocarbons (PAHs) and finally to soot, with its fused-ring, graphitic structure. It is anticipated that such growth will take place through an increasingly complex set of PAH intermediates. There have been several mechanisms proposed by which this growth can occur. For example, the second aromatic ring could be formed by successive additions of acetylene to the phenyl radical, in the so-called hydrogen abstraction acetylene addition (HACA) mechanism.[14,16,17] A variant on this theme is the addition of diacetylene to the phenyl radical to form a $C_{10}H_7$ adduct directly, which can rearrange to the naphthyl radical.[18] Alternatively, recombination of cyclopentadienyl radicals (C_5H_5) could also lead directly to naphthalene following hydrogen loss.[17,19−21] Additional studies to illuminate the possible pathways to the formation of substituted naphthalenes and higher order ring structures[22,23] have been undertaken to determine suitable mechanisms for further growth of PAHs in flames.

Motivated by the formation of benzene from C_4H_2* + 1,3-butadiene, we have recently extended our studies to include the reactions of C_4H_2* with the aromatic molecules themselves, initially focusing attention on benzene and toluene.[24] The present study builds on that work by extending it to include the reaction of C_4H_2* with styrene. A primary motivation for our work is to determine whether C_4H_2* can react with styrene to form naphthalene, a first fused aromatic product. The similar bonding arrangements of 1,3-butadiene and styrene would lead one to believe that such a route might indeed occur.

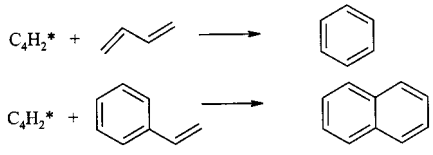

As we shall see, the major products of C_4H_2* + styrene include species with molecular formulas $C_{10}H_8$ and $C_{12}H_8$, the former being consistent with naphthalene. However, styrene possesses many sites for attack of C_4H_2*, leading to several alternative $C_{10}H_8$ structural isomers besides naphthalene, includ-

* Author to whom correspondence should be addressed. Fax: (765) 494-0239. E-mail: zwier@purdue.edu.

10.1021/jp014502q CCC: $22.00
Published on Web 05/23/2002

ing *o*- **(I)**, *m*- **(II)**, and *p*-ethynyl styrene **(III)**, and 1-phenyl-1-buten-3-yne **(IV)**: A major challenge of the present work, then,

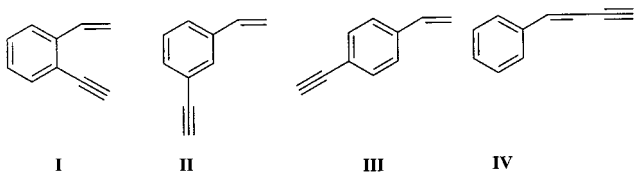

is to spectroscopically characterize the observed products in order to make structural identifications. Using UV−UV holeburning spectroscopy, we identified **II** and **IV** as photoproducts, while naphthalene was not detected. We conclude that naphthalene is not formed in significant quantities in the $C_4H_2^*$ + styrene reaction on the time scale of the present experiment.

II. Experimental Section

The experimental apparatus used in this work has been described previously.[9] The reaction mixture is prepared by passing diacetylene (5−7% in helium) over styrene in a stainless steel reservoir to pick up the sample at its vapor pressure (6 Torr), giving a concentration of styrene in the C_4H_2/He mixture of less than 1% at 30 psig backing pressure. The gas mixture passes through a pulsed valve (R. M. Jordan Co.) operating at 10 Hz, producing 100−200 μs long gas pulses at a total flow rate of 1−2 standard cm^3/min.

To study only the primary products that result from the reaction of metastable diacetylene with styrene, the reactant mixture is pulsed into a short reaction tube (1 cm long, 2 mm I.D.). While the reactant mixture is in the tube, photochemistry is initiated using the doubled output (0.7 mJ/pulse) of a Nd:YAG pumped KTP/BBO optical parametric converter (LaserVision) tuned to the $2^1_0 6^1_0$ of the $^1\Delta_u \leftarrow X^1\Sigma^+_g$ transition in diacetylene (231.5 nm).[8] We estimate that approximately 2−3% of the diacetylene in the tube is photoexcited, on the basis of the absorption cross-section of diacetylene (80 cm^{-1} atm^{-1}) determined by Glicker and Okabe.[25] The excited diacetylene then undergoes rapid intersystem crossing from the excited singlet state, either directly or mediated by the lower energy $^1\Sigma_u$+ state, to produce high vibrational levels of the low-lying triplet states ($^3\Delta_u$ and/or $^3\Sigma_u$+).[9,25] Reaction of the metastable diacetylene occurs in parallel with vibrational relaxation in the triplet manifold during the 20 μs traversal of the gas mixture in the tube. After the gas exits the tube, free expansion into the vacuum chamber quenches any further reaction, limiting the formation of secondary products.

The gas mixture is ionized approximately 7 cm from the exit of the reaction tube in the ion extraction region of a time-of-flight mass spectrometer using one of three photoionization schemes: vacuum ultraviolet (VUV) ionization, resonant two-photon ionization (R2PI), or UV−UV holeburning. VUV photoionization with 118 nm (10.5 eV) photons produced by tripling the third harmonic of a Nd:YAG laser in a xenon/argon gas mixture[9,26] provides general mass analysis. Ultraviolet spectra of the photoproducts are recorded using R2PI over the wavelength range 600−570 nm (typical for the aromatic derivatives seen in these experiments) using the doubled the output (0.8 mJ/pulse) of a Nd:YAG pumped dye laser in three dye regions (Rhodamine 6G, 590, 610).

UV−UV holeburning is an example of the general class of holeburning techniques[27,28] that enables the deconvolution of an R2PI spectrum composed of vibronic structure from several isomers into sub-spectra of the individual species present. A relatively high-power dye laser (1 mJ/pulse), operated at 5 Hz, is fixed on a particular feature in the composite R2PI spectrum. The function of this holeburn laser (ω_{HB}) is to remove population from the ground state of the species from which the transition originates. After an approximately 200 ns delay, a second, lower-power dye laser (0.3 mJ/pulse) firing at 10 Hz is scanned through the R2PI spectrum of the desired photoproduct. The two lasers are fired at different repetition rates to use an active baseline subtraction technique, in which the difference in ion signal between successive shots (one with both lasers, one with only the probe laser) is monitored. When the probe laser is resonant with a vibronic transition coming from the same ground state as ω_{HB}, that transition will appear as a depletion in the holeburn spectrum.

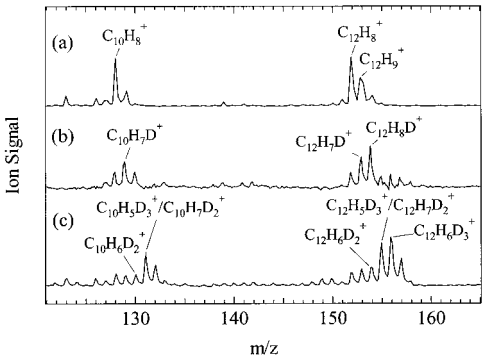

Figure 1. VUV photoionization difference mass spectra highlighting the photoproducts for the reactions (a) $C_4H_2^* + C_8H_8$, (b) $C_4D_2^* + C_8H_8$, and (c) $C_4H_2^* + C_8H_5D_3$. The reactant mass peaks are 100 to 200 times larger than the photoproduct peaks and are not shown. Signal from the fully nondeuterated reaction is present in the two deuterated cases due to residual nondeuterated sample in the gas handling system.

Styrene and deuterated styrene-d_3 (deuteration of the vinylic group) were used as supplied (Aldrich; 99+% and 98% atom D purity, respectively). Diacetylene and deuterated diacetylene were synthesized in our laboratory using methods described previously.[9,10] *m*-Ethynyl styrene and 1-phenyl-3-buten-1-yne were synthesized at Purdue University using standard procedures.[29,30]

III. Results

A. VUV Photoionization Studies. To highlight the mass peaks due to the photoproducts, the mass spectra reported in this paper are the difference between a mass spectrum taken with the photoexcitation laser on and one taken with the photoexcitation laser off. The molecular formulas in the spectra were determined from the mass-to-charge ratios of the respective peaks. Figure 1a shows a difference mass spectrum from the reaction of a 5:1 mixture of diacetylene and styrene, where the reactant mixture ratio was determined from the peak areas of the primary ions in the VUV mass spectra (assuming equal photoionization cross-sections at 118 nm).

The two reactant peaks (not shown in the figure), C_4H_2 (m/z = 50) and C_8H_8 (m/z = 104), are about 100 to 200 times more intense than the photoproduct peaks. To sensitively detect the photoproducts, a high voltage pulse (+800 V) is applied to a deflection plate in the flight tube to repel only the reactant ions away from the microchannel plate. A double pulse was applied to repel both the diacetylene and styrene ions while still detecting ions with masses between the two primary ions. However, no diacetylene plus styrene photoproducts were observed below the mass of styrene. Previous studies of poly-yne, enyne, cumulene,[11] and aromatic molecules[12] have shown no evidence of fragmentation upon 118 nm ionization, consistent with the study of Arps et al.[31] of a range of organic molecules. Therefore,

TABLE 1: Percent Product Yields[a,b] for Metastable Diacetylene Reacting with Styrene Corresponding Isotopic Reactions

$C_4H_2^* + C_8H_8$		$C_4D_2^* + C_8H_8$		$C_4H_2^* + C_8H_5D_3$	
$C_{10}H_6$	4%	$C_{10}H_5D$	7%	$C_{10}H_6$	4%
$C_{10}H_7$	4%	$C_{10}H_6D$	12%[c]	$C_{10}H_7$	3%
$C_{10}H_8$	26%	$C_{10}H_7D$	20%	$C_{10}H_6D_2$	6%
				$C_{10}H_5D_3/C_{10}H_7D_2$	16%
$C_{10}H_9$	10%	$C_{10}H_8D$	11%	$C_{10}H_6D_3$	10%
$C_{12}H_8$	33%	$C_{12}H_7D$	22%	$C_{12}H_6D_2$	11%
				$C_{12}H_5D_3/C_{12}H_7D_2$	23%
$C_{12}H_9$	23%	$C_{12}H_8D$	28%	$C_{12}H_6D_3$	27%

[a] Percent product yields were determined from the integrated peak areas in the difference mass spectrum. [b] Estimated error on the percent yields is ±3%. [c] This product yield is slightly high due to the interference of a small percentage of nondeuterated photoproduct, $C_{10}H_8$, at this mass.

we assume throughout this paper that the species in the difference mass spectra represent the nascent, neutral products formed in the gas-phase reaction.

The three major photochemical product peaks observed for the $C_4H_2^* + C_8H_8$ reaction (Figure 1a) occur at $m/z = 128$ ($C_{10}H_8$), $m/z = 152$ ($C_{12}H_8$), and $m/z = 153$ ($C_{12}H_9$). Minor products of the reaction have mass-to-charge ratios $m/z = 126$ ($C_{10}H_6$), $m/z = 127$ ($C_{10}H_7$), and $m/z = 129$ ($C_{10}H_9$). The percent product yields are given in Table 1. The reaction of $C_4H_2^*$ with ground-state C_4H_2 naturally occurs in parallel with the reaction with styrene, so the suite of reactions occurring in the reaction tube is as follows:

$$C_4H_2^* + C_4H_2 \rightarrow C_6H_2 + (C_2H_2) \quad k_{C_6H_2} \tag{1a}$$

$$\rightarrow C_8H_2 + (H_2 \text{ or } 2H) \quad k_{C_8H_2} \tag{1b}$$

$$\rightarrow C_8H_3 + (H) \quad k_{C_8H_3} \tag{1c}$$

$$C_4H_2^* + C_8H_8 \rightarrow C_{10}H_8 + (C_2H_2) \quad k_{C_{10}H_8} \tag{2a}$$

$$\rightarrow C_{12}H_8 + (H_2 \text{ or } 2H) \quad k_{C_{12}H_8} \tag{2b}$$

$$\rightarrow C_{12}H_9 + (H) \quad k_{C_{12}H_9} \tag{2c}$$

$$\rightarrow C_{10}H_6 + (C_2H_4) \quad k_{C_{10}H_6} \tag{2d}$$

$$\rightarrow C_{10}H_7 + C_2H_3 \quad k_{C_{10}H_7} \tag{2e}$$

$$\rightarrow C_{10}H_9 + (C_2H) \quad k_{C_{10}H_9} \tag{2f}$$

The products of the diacetylene/diacetylene reaction are not shown in Figure 1a. The C_6H_2 and C_8H_2 products have been shown to be triacetylene and tetracetylene, respectively, in earlier work.[32] The products listed in parentheses have ionization potentials greater than 10.5 eV, so they are not detected using 118 nm VUV photoionization.

To make certain that the photoproducts are consistent with primary, gas-phase species created by the excitation of diacetylene, two checks were carried out, as in earlier studies.[8−12,24] First, action spectra (not shown) of the photoproducts were recorded by tuning the photoexcitation laser through the $2^1_0 6^1_0$ transition of diacetylene. All of the photoproducts track the absorption curve of the $2^1_0 6^1_0$ transition, establishing that they are produced only following the excitation of diacetylene. Second, scans varying the time between the photoexcitation laser and the ionization laser (also not shown) were carried out to ensure that the observed photoproducts have arrival times consistent with primary, gas-phase photoproducts uncompromised by wall reactions. In such a reaction time scan, the VUV photoionization laser is fixed in time relative to the pulsed valve, while the photoexcitation laser time is scanned. The distribution of the photoproducts in time is roughly Gaussian in shape with full width at half-maximum (fwhm) of about 20 microseconds. It peaks at an arrival time corresponding to the traversal time of the molecules from the reaction tube to the ion source region. The form of the distribution was the same for all of the $C_4H_2^* + C_8H_8$ photoproducts. As a final check, mass spectra were recorded following excitation at the wavelength of the $2^1_0 6^1_0$ transition while only styrene was present in the expansion, as styrene has significant structureless absorption in this region. No photoproducts were detected, indicating that styrene/styrene reactions do not contribute to the observed photoproducts.

To gain further insight into the pathways of the $C_4H_2^* + C_8H_8$ reaction, deuterium labeling studies were conducted. Figure 1(b) and (c) show the difference mass spectra for the $C_4D_2^* + C_8H_8$ and the $C_4H_2^* + C_8H_5D_3$ reactions, respectively. The mass spectrum showing the photoproducts of $C_4D_2^* + C_8H_8$ (Figure 1(b)) has been corrected to remove features from residual $C_4H_2^* + C_8H_5D_3$ photochemistry. Percent product yields for these reactions are given in Table 1. In the reaction involving the deuterated diacetylene, the masses of the major photoproducts increased by only one mass unit, consistent with one deuterium atom from C_4D_2 being retained in the observed products.

$$C_4D_2^* + C_8H_8 \rightarrow C_{10}H_7D + (C_2HD) \tag{3a}$$

$$\rightarrow C_{12}H_7D + (HD \text{ or } H + D) \tag{3b}$$

$$\rightarrow C_{12}H_8D + (D) \tag{3c}$$

$$\rightarrow C_{10}H_5D + (C_2H_3D) \tag{3d}$$

$$\rightarrow C_{10}H_5D_2 + C_2H_3 \tag{3e}$$

$$\rightarrow C_{10}H_8D + (C_2D) \tag{3f}$$

The minor product at $m/z = 126$ in the undeuterated reaction shifts one mass unit to $m/z = 127$ upon deuteration of the diacetylene. This is consistent with the elimination of C_2H_3D from the reaction complex. However, due to the presence of features resulting from the reaction of $C_4H_2^*$ with residual undeuterated styrene, the data is inconclusive as to whether the minor product at $m/z = 127$ shifts one or two mass units upon deuteration of the diacetylene. If the vinylic group is eliminated, as indicated in eq 3e, one would expect a shift of two mass units for this product.

The reaction of $C_4H_2^* + C_8H_5D_3$ (Figure 1c) proved to be more illuminating in the determination of product structures. The three vinylic hydrogens on styrene are deuterium labeled, while the ring hydrogens remain unlabeled. We assume that an

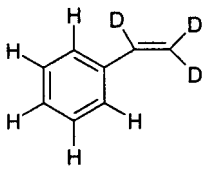

attack on the ring would leave the deuterated vinyl group intact, while attack at the vinyl group would lead to a loss of deuterium, shifting the major photoproducts by three or two mass units,

respectively. Masses corresponding to attack at both sites were observed in the VUV mass spectrum. For the case of diacetylenic attack on the ring portion of styrene, the set of reactions is given by

$$C_4H_2^* + C_8H_5D_3 \rightarrow C_{10}H_5D_3 + (C_2H_2) \quad (4a)$$

$$\rightarrow C_{12}H_5D_3 + (H_2 \text{ or } H + H) \quad (4b)$$

$$\rightarrow C_{12}H_6D_3 + (H) \quad (4c)$$

$$\rightarrow C_{10}H_6 + (C_2HD_3) \quad (4d)$$

$$\rightarrow C_{10}H_7 + C_2D_3 \quad (4e)$$

$$\rightarrow C_{10}H_6D_3 + (C_2H) \quad (4f)$$

The appearance of photoproducts at masses 126 and 127 (reactions 4d and 4e) would indicate that these minor products are unaffected by the deuterium substitution on the vinylic group, pointing toward the leaving of the vinyl group as the mechanism for the formation of these two products. In the case of attack on the vinyl group, the suite of reactions is as follows:

$$C_4H_2^* + C_8H_5D_3 \rightarrow C_{10}H_6D_2 + (C_2HD) \quad (5a)$$

$$\rightarrow C_{12}H_6D_2 + (HD \text{ or } H + D) \quad (5b)$$

$$\rightarrow C_{12}H_7D_2 + (D) \quad (5c)$$

$$\rightarrow C_{10}H_6 + (C_2HD_3) \quad (5d)$$

$$\rightarrow C_{10}H_7 + C_2D_3 \quad (5e)$$

$$\rightarrow C_{10}H_7D_2 + (C_2D) \quad (5f)$$

The appearance of a small peak at $m/z = 130$ in the VUV difference mass spectrum indicates that the $C_{10}H_6D_2$ (reaction 5a) product is formed through attack on the vinylic group. As will be discussed in Section III.B, R2PI spectra were recorded for photoproduct species at both masses 130 and 131 in the $C_4H_2^* + C_8H_5D_3$ reaction, confirming the two distinct reaction pathways. While it appears that the peak at $m/z = 131$ is of much greater intensity than the peak at $m/z = 130$, both the minor product $C_{10}H_7D_2$ from the vinylic attack and the major product $C_{10}H_5D_3$ from the ring attack contribute to the ion signal in the former channel. Thus we cannot draw firm conclusions regarding the relative product ratios for the different species in the VUV spectrum, nor can we make any estimates of the branching ratio for the two different reaction channels.

B. R2PI Studies. Most of the photoproducts observed in the VUV mass spectra can exist in any one of several possible structural isomers. Therefore, UV spectra were recorded using R2PI to obtain structural information about the major products, $C_{10}H_8$ (Figure 2a) and $C_{12}H_8$ (Figure 2b). Several possible isomers are considered likely candidates for $C_{10}H_8$ photoproducts, including *o*-, *m*-, and *p*-ethynyl styrene (**I**−**III**) (resulting from an attack on the ring) and 1-phenyl-1-buten-3-yne (**IV**) (from an attack on the vinylic group). All of these species are anticipated to have $S_1 \leftarrow S_0$ transitions in the near UV. As mentioned, R2PI spectra of the deuterated photoproducts corresponding to the $C_{10}H_8$ photoproducts were also recorded. Figure 3 shows the R2PI spectrum of the nondeuterated $C_{10}H_8$ product (a) compared with those for $C_{10}H_6D_2$ (b) and $C_{10}H_5D_3$ (c), all recorded simultaneously. The $C_{10}H_6D_2$ species has a different origin than the $C_{10}H_5D_3$ species, suggesting that there are at least two different isomeric species in the $C_{10}H_8$ photoproduct channel produced by distinctly different mechanisms. These origins have been labeled A and B in the undeuterated spectrum.

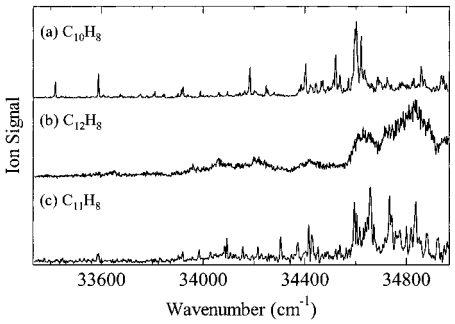

Figure 2. One-color R2PI from $C_4H_2^* + C_8H_8$ of the (a) $C_{10}H_8$ photoproduct, (b) $C_{12}H_8$ photoproduct, and (c) $C_{11}H_8$ photoproduct.

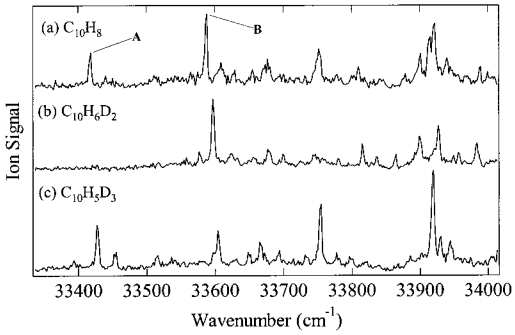

Figure 3. One-color R2PI of (a) the $C_{10}H_8$ photoproduct from $C_4H_2^* + C_8H_8$, (b) the $C_{10}H_6D_2$ photoproduct from $C_4H_2^* + C_8H_5D_3$, and (c) the $C_{10}H_5D_3$ photoproduct from $C_4H_2^* + C_8H_5D_3$.

In addition to the two main photoproducts, an additional minor photoproduct was observed by R2PI that was not visible in the VUV mass spectra. A peak at $m/z = 140$ ($C_{11}H_8$) appeared in the region where we were looking for the two major photoproducts (Figure 2c). The origin for this species is tentatively assigned at 33589 cm^{-1}, with strong vibronic bands appearing 331, 396, and 506 cm^{-1} above the origin. This species had an action spectrum which followed the $2^1_0 6^1_0$ transition and a reaction time scan consistent with a primary photoproduct. The species (probably an aromatic derivative) clearly has a large enough R2PI cross-section to be detected in trace amounts, but was not present in sufficient quantities to be detected by VUV ionization. R2PI spectra were recorded in the $m/z = 141$ and $m/z = 143$ mass channels for the reaction of $C_4H_2^* + C_8H_5D_3$, again suggesting at least two different isomers, one of which involves loss of CD_2. It was not possible to make a structural determination for the $C_{11}H_8$ product, nor for the $C_{12}H_8$ product, largely because authentic samples of the likely isomers were not available.

C. UV−UV Holeburning Studies. UV−UV holeburning scans were taken at the two probable origins (A and B) in the $C_{10}H_8$ photoproduct R2PI spectrum. Figure 4(b) shows the spectrum taken while the holeburning laser was tuned to origin A farthest to the red (33418 cm^{-1}). Figure 5(b) shows the spectrum taken with the holeburning laser tuned to origin B (33587 cm^{-1}). The majority of the peaks in the overall $C_{10}H_8$ photoproduct R2PI spectrum are duplicated in either the A or the B R2PI spectra, with one notable exception. The peak at 34622 cm^{-1} in the photoproduct spectrum (marked with an asterisk in Figures 4 and 5) is not clearly associated with either of the holeburn spectra, leaving open the possibility of a third

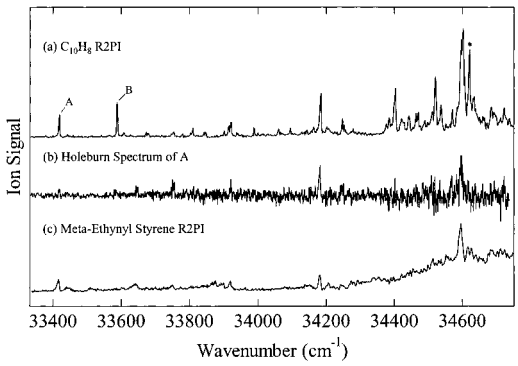

Figure 4. (a) One-color R2PI of the $C_{10}H_8$ photoproduct from C_4H_2* + C_8H_8 with the two holeburning orgins labeled. (b) UV−UV holeburning spectrum obtained by holeburning the peak of the $C_{10}H_8$ photoproduct designated A. (c) R2PI spectrum of *m*-ethynyl styrene seeded in helium taken under conditions similar to those used for the photochemistry.

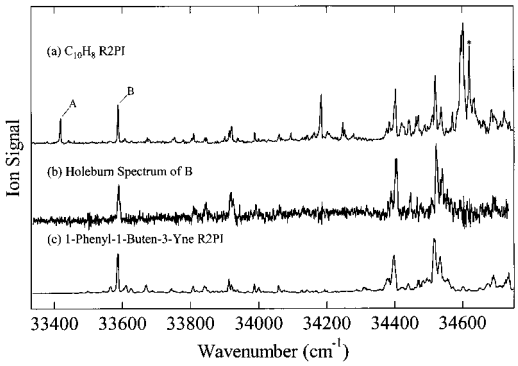

Figure 5. (a) One-color R2PI of the $C_{10}H_8$ photoproduct from C_4H_2* + C_8H_8 with the two holeburning origins labeled. (b) UV−UV holeburning spectrum obtained by holeburning the peak of the $C_{10}H_8$ photoproduct designated B. (c) R2PI spectrum of 1-phenyl-1-buten-3-yne seeded in helium taken under conditions similar to those used for the photochemistry.

origin; we were not able to further characterize this spectrum due to congestion from the other species in this region. However, UV−UV holeburning confirmed that there are at least two distinct components present in the composite spectrum of the $C_{10}H_8$ photoproduct, one with origin A and one with origin B.

To associate these spectra with specific product structures, it was necessary to obtain known samples of the likely species identified above as potential photoproducts. None of these are available commercially, so a custom synthesis was undertaken here at Purdue University.[29,30] The R2PI spectra of 1-phenyl-1-buten-3-yne and *m*-ethynyl styrene are shown in Figures 4(c) and 5(c), respectively. Peak-to-peak comparisons show that species A is *m*-ethynyl styrene, and that species B is 1-phenyl-1-buten-3-yne. The *m*-ethynyl styrene spectrum has poor signal-to-noise due to the small vapor pressure of the impure sample. Samples *of o*- and *p*-ethynyl styrene samples were unavailable at the time of this study, so their presence in the $C_{10}H_8$ photoproduct cannot be confirmed, although previous work suggests that they are both also likely products.[24] Naphthalene was ruled out as a photoproduct on the basis of the R2PI data. The naphthalene origin (32020.2 cm^{-1}) cannot be observed in one-color R2PI, as the ionization potential of naphthalene is too large (IP = 8.144 eV), but there are several vibronic transitions (most notably bands at 32930 and 33155 cm^{-1})[33] which can be observed in one-color R2PI to the red of the A origin of the $C_{10}H_8$ photoproduct. Scans as far red as 610 nm showed no trace of structure in the m/z = 128 mass channel beyond the A origin.

IV. Discussion

A. Percent Product Yields. The percent product yields extracted from the difference mass spectra are given in Table 1. The distributions of products formed from nondeuterated and deuterated reactants are fairly consistent. In the C_4H_2* + $C_8H_5D_3$ reaction, the major photoproduct analogues to $C_{10}H_8$ and $C_{12}H_8$ are split between the two attack sites. The $C_{10}H_8$ goes to $C_{10}H_6D_2$ and $C_{10}H_5D_3$ with the latter having a greater percentage at least in part because the minor photoproduct $C_{10}H_7D_2$ also has that same mass. For this reason, it is impossible to make any generalizations about which attack site is favored. The $C_{12}H_8$ product mass is split between the $C_{12}H_6D_2$ and $C_{12}H_5D_3$ products, again with a minor contribution from $C_{12}H_7D_2$ in the $C_{12}H_5D_3$ mass channel.

In the styrene reaction, the radical channel $C_{12}H_9$ + H is a major channel, which differs from the reactions of diacetylene with benzene and toluene, where loss of a single hydrogen from the reaction complex was a minor product.[24] In the reaction of diacetylene with itself, it was found that the C_8H_3 product increased in intensity relative to C_8H_2 when nitrogen was used as a buffer gas instead of helium.[9] The loss of two hydrogen atoms (C_4H_2* + C_4H_2 → C_8H_2 + 2H) requires about 40 kcal/mol more than the loss of a single hydrogen (C_4H_2* + C_4H_2 → C_8H_3 + H), and is just about 20 kcal/mol below the energy added to the system in the photoexcitation. Nitrogen is more effective in deactivating diacetylene to low-lying vibrational levels of the triplet state, dropping the energy available in the C_4H_2* below the threshold for elimination of two hydrogen atoms from the reaction complex and thus favoring C_8H_3 formation. In the reaction of diacetylene with styrene (in helium), styrene may also be collisionally deactivating the diacetylene vibrations. Difference mass spectra show that the C_8H_3 product is increased relative to the C_8H_2 product when the styrene reactant is present. This deactivation would explain the unusual appearance of $C_{12}H_9$ as a major photoproduct.

To convert the observed product yields into quantitatively accurate quantum yields, the ion signal data need to be corrected for differences in absolute photoionization efficiencies at 118 nm. However, photoionization cross-sections are not available for the array of unusual photoproducts studied here. However, as the products have similar chemical structures, they are expected to have similar photoionization cross-sections at 118 nm. The percent product yields in Table 1 are reported under this assumption.

B. Relative Rate Constants. The reaction of metastable diacetylene with styrene was carried out under early-time conditions where primary products dominate and secondary reactions are negligible. With the assumption that the photoproducts have similar photoionization cross-sections, a psuedo first-order kinetic model can be used to extract an effective rate constant for the reaction under study relative to the C_4H_2* + C_4H_2 reaction which occurs in parallel.[11] Figure 6 shows a plot of the integrated intensity ratio of the product ion intensities from the C_4H_2* + C_8H_8 reaction to those from the C_4H_2* + C_4H_2 reaction versus the integrated intensity ratio of the styrene to diacetylene primary ion signals. The plot gives a straight line with a slope equal to the rate constant ratio. The ratio obtained is $k_{C_8H_8}/k_{C_4H_2} = 1.95 \pm 0.18$, where the error bars represent one standard deviation on the mean. The relative rate constant for the reaction of metastable diacetylene with styrene is considerably larger than those previously obtained in studies of C_4H_2* reactions with small, aliphatic hydrocarbons,[9−12] but is quite similar to the rate constants from the reaction of metastable diacetylene with the aromatics benzene and toluene.[24]

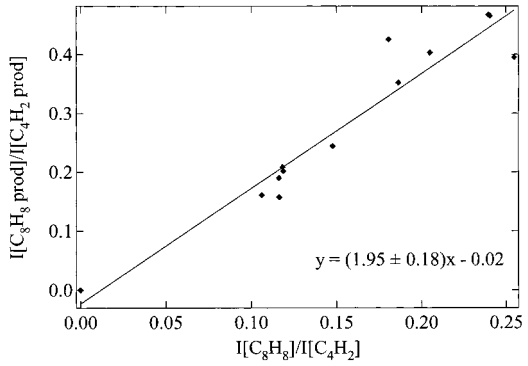

Figure 6. Concentration study for the reaction $C_4H_2^* + C_8H_8$. Plotted are the ratio of product ion intensities $I[C_8H_8$ products$]/I[C_4H_2$ products] versus the ratio of reactant ion intensities $I[C_8H_8]/I[C_4H_2]$. The slope of the line fit to these points gives the relative rate constant for the reaction, $k_{C_8H_8}/k_{C_4H_2} = 1.95$.

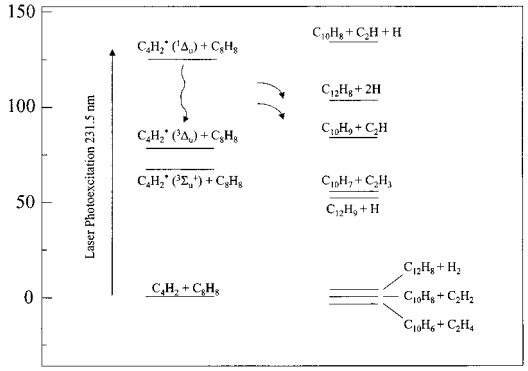

Figure 7. Thermodynamic energetics for the reaction $C_4H_2^* + C_8H_8$. See Tables 2 and 3 for more detail.

TABLE 2: Heats of Formation for the Various Photoproducts

species	ΔH_f (kcal/mol) at 298 °C	ref
H	52.103 ± 0.001	40
H_2	0	
C_2H	135.1 ± 0.7	40
C_2H_2	54.35 ± 0.19	41
C_2H_3	71 ± 1	42
C_2H_4	12.54 ± 0.07	43
C_4H_2 (diacetylene)	111 ± 2	36
C_8H_8 (styrene)	35.11 ± 0.24	44
$C_{10}H_6$ (phenyldiacetylene)	133 ± 3	45
$C_{10}H_8$[a]	93 ± 4	45
$C_{10}H_8$ (naphthalene)	36.12 ± 0.45	43
$C_{12}H_8$[a]	148 ± 4	45

[a] This value is an average ΔH_f for the different structures. Benson's method predicts that the ortho, meta, and para $C_{10}H_8$ isomers (94.3, 93.7, and 93.7 kcal/mol, respectively) and the 1-phenyl-1-buten-3-yne (91.9 kcal/mol) are very close in value.

C. Energetics of the Reactions. Figure 7 shows an approximate energy level diagram for the diacetylene plus styrene reaction. The heats of formation for the various photoproducts (see Table 2) are used to calculate heats of reaction (see Table 3) relative to the two ground-state reactant molecules. Diacetylene is initially given 123.5 kcal/mol of energy when it is excited to the $2^1_0 6^1_0$ level of the $^1\Delta_u$ state, but the precise energy available for the reaction from the triplet state depends on the degree of vibrational deactivation in the triplet manifold.

There are several aspects of the reaction energetics that are worth highlighting. First, for any of the possible $C_{10}H_8$ product isomers, the C_2H_2 coproduct must be formed intact as acetylene,

TABLE 3: Heats of Reaction for the Various Photoproduct Reactions

reaction[a,b]	ΔH_{rxn} at 298 °C (kcal/mol)
$C_4H_2 + h\nu$ (231.5 nm) → $C_4H_2^*$	123.5
$C_4H_2 + C_8H_8 \rightarrow C_{10}H_6 + (C_2H_4)$	−1 ± 7
$C_4H_2 + C_8H_8 \rightarrow C_{10}H_7 + C_2H_3$	58 ± 7
$C_4H_2 + C_8H_8 \rightarrow C_{10}H_8 + (C_2H + H)$	134 ± 10
$C_4H_2 + C_8H_8 \rightarrow C_{10}H_8 + (C_2H_2)$	1 ± 10
$C_4H_2 + C_8H_8 \rightarrow$ naphthalene + (C_2H_2)	−56 ± 3
$C_4H_2 + C_8H_8 \rightarrow C_{10}H_9 + (C_2H)$	82 ± 10
$C_4H_2 + C_8H_8 \rightarrow C_{12}H_8 + (2H)$	106 ± 10
$C_4H_2 + C_8H_8 \rightarrow C_{12}H_8 + (H_2)$	2 ± 10
$C_4H_2 + C_8H_8 \rightarrow C_{12}H_9 + (H)$	54 ± 10

[a] The products listed in parentheses are not directly detected in the present work. [b] The product structures are those indicated in Table 2.

as the energy is not available to give $C_{10}H_8$ and C_2H and H. Second, formation of naphthalene is favored over either the ethynyl styrenes or the 1-phenyl-1-buten-3-yne by roughly 60 kcal/mol, yet it is not observed as a photoproduct. Third, the energy is available for the $C_{12}H_8$ product to be formed with loss of either H_2 of 2H, depending on the degree of vibrational deactivation of $C_4H_2^*$. However, the relative intensity of the $C_{12}H_9$ peak to the $C_{12}H_8$ peak in the VUV mass spectrum suggests that vibrational deactivation minimizes the loss of two hydrogen atoms. Finally, while elimination of the vinyl group (either with a hydrogen as C_2H_4 or alone as C_2H_3) from the ring is energetically comparable to some of the other observed product channels, these species are formed only as minor products in the reaction. This difference may arise from mechanistic effects, as discussed below.

D. Reaction Mechanisms. The isotopic R2PI spectra and the UV−UV holeburning spectra clearly show that there are at least two distinct isomers of $C_{10}H_8$ formed in the reation of metastable diacetylene with styrene. As it is unlikely that one intermediate could produce both a di-substituted ring product and a product from addition to the vinylic group, we postulate that there are two distinct attack sites for the diacetylene, with *m*-ethynyl styrene resulting from an attack on the ring, and 1-phenyl-1-buten-3-yne resulting from an attack on the vinylic group. The energetics dictate that loss of C_2H_2 (C_2HD) must happen in a concerted fashion from the reaction complex in either mechanism. An analogous concerted loss of H_2 (HD) seems plausible as well. Both mechanisms must also account for the mass shifts observed in the deuterium labeling experiments, particlarly with respect to the loss of H or D in the deuterated styrene reaction. In the two mechanisms presented below, $C_4D_2^*$ is shown as the reactant rather than $C_4H_2^*$ in order to distinguish the styrene and diacetylene hydrogens. The metastable state of diacetylene is represented as a cumulene diradical, based on the calculations of Karpfen and Lischka[34] and Vila et al.[35]

A mechanism for the formation of 1-phenyl-1-buten-3-yne following vinylic attack is given in Figure 8. The $C_4H_2^*$ attack at the double bond of the vinylic group produces **1**, which rearranges to give **2**, presented in two different forms. From intermediate **2a**, the complex can eliminate C_2HD to give **3**, which rearranges to 1-phenyl-1-buten-3-yne **4**, or the complex loses C_2D to produce $C_{10}H_9$ **6**. The data does not suggest whether the 1-phenyl-1-butene-3-yne is in a cis or trans configuration or a combination of the two isomers. From **2b**, a simple elimination yields $C_{12}H_8$ (1-phenyl-1-hexen-3,5-diyne) **7** and $C_{12}H_9$ **8**. While only an attack at the terminal carbon of the vinylic chain leads to the observed photoproduct, an attack

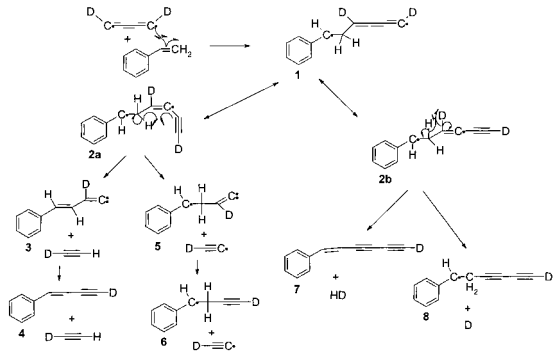

Figure 8. Proposed mechanism for the formation of 1-phenyl-1-buten-3-yne **4**, the $C_{10}H_9$ radical species **6**, 1-phenyl-1-hexen-3,5-diyne **7**, and the $C_{12}H_9$ radical species **8** from C_4H_2* + C_8H_8 from vinylic attack.

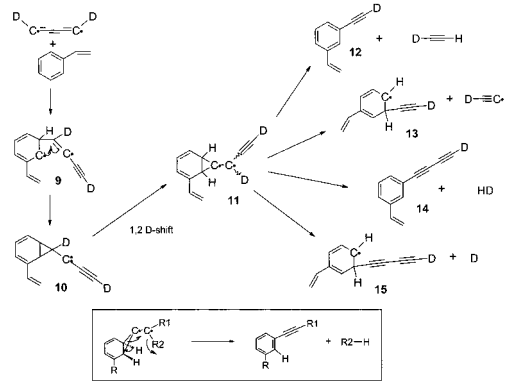

Figure 9. Proposed mechanism for the formation of *m*-ethynyl styrene **12**, the $C_{10}H_9$ radical species **13**, *m*-diethynyl styrene **14**, and the $C_{12}H_9$ radical species **15** from C_4H_2* + C_8H_8 from ring attack. The inset shows the details for the bond rearrangement of **11** to give the major reaction products.

at the interior carbon cannot be ruled out. Such an attack could result in a branched chain in the photoproduct, or it may lead to the elimination of the terminal CH_2, resulting in the minor $C_{11}H_8$ photoproduct detected via its R2PI spectrum.

For the mechanism describing the attack on the ring, we utilize a mechanism developed for previous diacetylene plus aromatic reactions.[24] This mechanism is shown in Figure 9. In the previous work of C_4H_2* + toluene, we found that statistical amounts of *o*-, *m*-, and *p*-ethynyl toluene were formed. In C_4H_2* + styrene, we have only identified *m*-ethynyl styrene, so the mechanism illustrates a meta attack by the radical on the ring producing **9**. Subsequently, the radical center on the ring attacks the double bond in the carbon chain, resulting in ring closure to a bicyclic carbene **10**. (This closure could happen to either the ortho position, as shown, or the para site.) A 1,2-deuterium shift then produces the key diradical intermediate **11**. This intermediate can eliminate along various paths to generate *m*-ethynyl styrene **12**, the $C_{10}H_9$ radical **13**, *m*-diethynyl styrene **14**, or the $C_{12}H_9$ radical **15**.

The mechanism presented in Figure 9 retains the triplet state character of the attacking C_4H_2* throughout much of the mechanism, including the formation of the triplet intermediate **11**. This intermediate has several advantages over its singlet counterpart.[24] First, the 1,2-deuterium shift should occur with greater ease in a triplet carbene than on a singlet manifold. Second, the bent triplet state of **11** brings the ring hydrogen close to the end of the carbon chain for the elimination step. It is clear that at some point during the mechanism, the products undergo intersystem crossing back to the singlet state, as we detect only singlet species in R2PI. The inset of Figure 9 shows the details of the six-electron elimination that intermediate **11** undergoes to generate the major products, where R1 and R2 can represent either a hydrogen or an acetylene unit.

As noted above, the cyclopropane bridge could form to either the ortho or para positions after meta attack. The possibility also exists that attack could occur at the ortho or para positions, with subsequent bridging to the adjacent sites. Once formed, the ring should open equally on either side. The mechanism thus predicts that the full range of ortho, meta, and para isomers should be produced, although the *m*-ethynyl styrene is the only ring-substituted isomer identified. In the mechanism for diacetylene plus toluene, the ortho substituted species was statistically favored after assuming attack only at the ipso, ortho, and para sites, as the methyl group is an ortho/para director. A vinylic group is not strongly activating or deactivating, so attack at any of the ring positions likely has equal probability. If attack at the ipso position were excluded on the basis of steric considerations, then a meta-substituted isomer would be statistically favored, as attack at any position can lead to opening at the meta site.

In the mechanisms presented here, the two minor products from C_4H_2* + C_8H_8 ($C_{10}H_6$ and $C_{10}H_7$) have been excluded. The deuterated data suggest that these two products are formed by elimination of the vinylic group, so the mechanism in Figure 8 (vinylic attack) does not seem likely to lead to either of these species. Their formation could result from attack at the ortho position on the ring, with the cyclopropane bridge forming to the ipso position. The elimination of the vinylic group in concert with a hydrogen atom from the attacking C_4H_2 would lead to the formation of the $C_{10}H_6$ product as phenyl diacetylene. It should also be noted that elimination of the vinylic group in concert with CH_2 would lead to the formation of phenyl acetylene (C_8H_6), which would appear at $m/z = 102$. These experiments could not detect a photoproduct at this mass due to interference from pulsing away styrene primary ion signal at $m/z = 104$.

Finally, we consider the $C_{11}H_8$ photoproduct seen only in R2PI. This product is unusual in that its formation involves the loss of CH_2 from the adduct. This likely accounts for its small product yield. In most of the C_4H_2* reactions we have studied, only stable reaction products such as acetylene, C_2H_4, or CH_4 are formed. The most reasonable location for loss of CH_2 from the vinylic group involves the terminal carbon, which suggests that the $C_{11}H_8$ photoproduct may result from vinylic attack at the interior carbon. It could also arise from an ortho ring attack, followed by a ring closure to the interior vinylic carbon (in concert with the loss of CH_2). This makes it notable despite its small yield, as it is the only photoproduct which seems likely to be a fused ring species. Two $C_{11}H_8$ isomers which are leading candidates for that observed experimentally are 2-ethynyl-1H-indene and 2-ethenylidene-2H-indene. So far, this species has

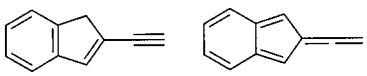

not been identified and we postulate no mechanism for its formation.

E. Implications for Flame Chemistry. The major products formed in this study, $C_{10}H_8$ and $C_{12}H_8$, are isomers of two of the most common PAHs found in sooting flames, naphthalene and acenaphthalene.[6,36] However, in this study, several distinctly less stable species are formed, and the creation of a second ring was not observed. A recent molecular beam TOF experiment by Guthe et al.[37] which studied the products of a benzene

discharge also showed no formation of the polycyclic compounds that are the end products of sooting flames. These authors postulate that since the discharge products were sampled early in formation, the more stable species seen in pyrolysis processes had not yet been formed. This same hypothesis could be applied to the primary photoproducts observed in this study of the reaction of metastable diacetylene and styrene. While naphthalene and acenaphthalene were not formed in this study, the fact that isomeric photoproducts of those species were formed is significant, particularly the 1-phenyl-1-buten-3-yne species. Zimmermann and co-workers have recently demonstrated the formation of naphthalene from 1-phenyl-1-buten-3-yne in flash vacuum photolysis.[38,39] Thus the reaction of C_4H_2* + styrene leads to aromatic derivatives which are readily isomerized to PAHs. It would be worthwhile to explore in more detail these isomerization pathways and their competition with reactions that lead away from PAHs to other products.

Acknowledgment. The authors gratefully acknowledge the Department of Energy, Office of Basic Energy Sciences, Division of Chemical Sciences for their support of this research under Grant No. DE-FG02-96ER14656. The authors also wish to acknowledge Professor John Grutzner for useful discussions on reaction mechanisms. Finally, the authors are indebted to Dr. H. Daniel Lee of Purdue University for synthesizing the 1-phenyl-1-buten-3-yne and *m*-ethynyl styrene.

References and Notes

(1) Bastin, E.; Delfau, J.-L.; Reuillon, M.; Vovelle, C.; Warnatz, J. *Twenty-second Symposium (International) on Combustion*, 1988.
(2) Lam, F. W.; Howard, J. B.; Longwell, J. P. *Twenty-second Symposium (International) on Combustion*, 1988; p 323.
(3) Melius, C. F.; Miller, J. A.; Evleth, E. M. *Twenty-fourth Symposium (International) on Combustion*, 1992; p 621.
(4) Miller, J. A.; Melius, C. F. *Combust. Flame* **1992**, *91*, 21.
(5) Shi, Y.; Ervin, K. M. *Chem. Phys. Lett.* **2000**, *318*, 149.
(6) Homann, K. H. *Twentieth Symposium (International) on Combustion*, 1984; p 857.
(7) Allan, M. *J. Chem. Phys.* **1984**, *80*, 6020.
(8) Bandy, R. E.; Lakshminarayan, C.; Frost, R. K.; Zwier, T. S. *Science* **1992**, *258*, 1630.
(9) Bandy, R. E.; Lakshminarayan, C.; Frost, R. K.; Zwier, T. S. *J. Chem. Phys.* **1993**, *98*, 5362.
(10) Frost, R. K.; Zavarin, G.; Zwier, T. S. *J. Phys. Chem.* **1995**, *99*, 9408.
(11) Frost, R. K.; Arrington, C. A.; Ramos, C.; Zwier, T. S. *J. Am. Chem. Soc.* **1996**, *118*, 4451.
(12) Arrington, C. A.; Ramos, C.; Robinson, A. D.; Zwier, T. S. *J. Phys. Chem. A* **1998**, *102*, 3315.
(13) McEnally, C. S.; Robinson, A. G.; Pfefferle, L. D.; Zwier, T. S. *Combust. Flame* **2000**, *123*, 344.
(14) McEnally, C. S.; Pfefferle, L. D. *Combust. Sci. Technol.* **1997**, *128*, 257.
(15) McEnally, C. S.; Pfefferle, L. D. *Combust. Flame* **1998**, *115*, 81.
(16) Wang, H.; Frenklach, M. *J. Phys. Chem.* **1994**, *98*, 11465.
(17) Marinov, N. M.; Pitz, W. J.; Westbrook, C. K.; Castaldi, M. J.; Senkan, S. M. *Combust. Sci. Technol.* **1996**, *116*, 211.
(18) Hausmann, M.; Homann, K.-H. *Ber. Bunsen-Ges. Phys. Chem.* **1997**, *101*, 651.
(19) Melius, C. F.; Colvin, M. E.; Marinov, N. M.; Pitz, W. J.; Senkan, S. M. *Twenty-sixth Symposium (International) on Combustion*, 1996; p 685.
(20) Castaldi, M. J.; Marinov, N. M.; Melius, C. F.; Huang, J.; Senkan, S. M.; Pitz, W. J.; Westbrook, C. K. *Twenty-sixth Symposium (International) on Combustion*, 1996; p 693.
(21) Friderichsen, A. V.; Shin, E. J.; Evans, R. J.; Nimlos, M. R.; Dayton, D. C.; Ellison, G. B. *Fuel* **2001**, *80*, 1747.
(22) Bapat, J. B.; Brown, R. F. C.; Bulmer, G. H.; Childs, T.; Coulston, K. J.; Eastwood, F. W.; Taylor, D. K. *Aust. J. Chem.* **1997**, *50*, 1159.
(23) Necula, A.; Scott, L. T. *J. Am. Chem. Soc.* **2000**, *122*, 1548.
(24) Robinson, A. G.; Winter, P. R.; Ramos, C.; Zwier, T. S. *J. Phys. Chem. A* **2000**, *104*, 10312.
(25) Glicker, S.; Okabe, H. *J. Phys. Chem.* **1987**, *91*, 437.
(26) Mahon, R.; Mcllrath, T. J.; Myerscough, V. P.; Koopman, D. W. *IEEE J. Quantum Electron.* **1979**, *6*, 444.
(27) Pribble, R. N.; Gruenloh, C. J.; Zwier, T. S. *Chem. Phys. Lett.* **1996**, *262*, 627.
(28) Scherzer, W.; Kratzchmar, O.; Selzle, H. L.; Schlag, E. W. *Z. Naturforsch. A* **1993**, *47*, 1248.
(29) Michel, P.; Gennet, D.; Rassat, A. *Tetrahedron Lett.* **1999**, 8575.
(30) Maeyama, K.; Iwasawa, N. *J. Org. Chem.* **1999**, *64*, 1344.
(31) Arps, J. H.; Chen, C. H.; McCann, M. P.; Datskou, I. *Appl. Spectrosc.* **1989**, *43*, 1211.
(32) Arrington, C. A.; Ramos, C.; Robinson, A. D.; Zwier, T. S. *J. Phys. Chem. A* **1999**, *103*, 1294.
(33) Beck, S. M.; Powers, D. E.; Hopkins, J. B.; Smalley, R. E. *J. Chem. Phys.* **1980**, *73*, 2019.
(34) Karpfen, A.; Lischka, H. *Chem. Phys.* **1986**, *102*, 91.
(35) Vila, F.; Borowski, P.; Jordan, K. D. *J. Phys. Chem. A* **2000**, *104*, 9009.
(36) Stein, S. E.; Fahr, A. *J. Phys. Chem.* **1985**, *89*, 3714.
(37) Guthe, F.; Ding, H.; Pino, T.; Maier, J. P. *Chem. Phys.* **2001**, *269*, 347.
(38) Schulz, K.; Hofmann, J.; Zimmermann, G. *Liebigs Ann./Recueil* **1997**, 2535.
(39) Hofmann, J.; Schulz, K.; Altmann, A.; Findeisen, M.; Zimmermann, G. *Liebigs Ann./Recueil* **1997**, 2541.
(40) Berkowitz, J.; Ellison, G. B.; Gutman, D. *J. Phys. Chem.* **1994**, *98*, 2744.
(41) Gurvich, L. V.; Veyts, I. V.; Alcock, C. B.; Iorish, V. S. *Thermodynamic Properties of Individual Substances*, 4th ed.; Hemisphere: New York, 1991; Vol. 2.
(42) Tsang, W. Heats of Formation of Organic Free Radicals by Kinetic Methods. In *Energetics of Organic Free Radicals*; Simoes, J. A. M., Greenburg, A., Liebman, J. F., Eds.; Blackie Academic and Professional: London, 1996.
(43) Chase, M. W., Jr. NIST-JANAF Thermochemical Tables. In *J. Phys. Chem. Ref. Data*, 4th ed., 1998; Vol. Monograph 9.
(44) Prosen, E. J.; Rossini, F. D. *J. Res. NBS* **1945**, *34*, 59.
(45) Benson, S. W. *Thermochemical Kinetics*, 2nd ed.; John Wiley & Sons: New York, 1976. Heats of formation for compounds for which no literature value could be found were estimated using Benson's Method of Group Additivity. Benson provides no group value for $C_t-(C_t)$, so the group $C_t-(C)$ was used instead. The uncertainties listed represent estimates.